SSRG International Journal of Electrical and Electronics Engineering
ISSN: 2348-8379/ https://doi.org/10.14445/23488379/IJEEE-V12I10P117

Volume 12 Issue 10, 232-245, October 2025

Original Article

Fuzzy Control Design for Steering and Speed in Autonomous Agricultural Vehicles: A Multibody Simulation Study

Gabriel Moreano[1*], Sergio Villacrés[2], Cristian Redrobán[2], Mayra Viscaino[3]

[1]*Departamento de Eléctrica, Electrónica y Telecomunicaciones, Universidad de las Fuerzas Armadas - ESPE, Latacunga, Ecuador.*
[2]*Facultad de Ingeniería Mecánica, Escuela Superior Politécnica de Chimborazo, Riobamba, Ecuador.*
[3]*Facultad de Ingeniería, Universidad Técnica de Ambato, Ambato, Ecuador.*

**Corresponding Author: gabriel.moreano.epn@gmail.com*

Received: 12 August 2025 Revised: 14 September 2025 Accepted: 17 October 2025 Published: 30 October 2025

Abstract - *For the agricultural industry, plants and crops are not uniformly distributed in terms of their species populations or physical structure. The autonomous vehicles for agricultural farming should have adaptive control which is able to handle soil variation and environmental variations. The scope of this work was to design a non-linear controller for an agricultural vehicle based on fuzzy logic and its simulation through a multi-body model. The major purpose was to establish the vehicle multi-body model, verify that the fuzzy control is efficient for this non-analyzed formula, as well as estimate its coherence with the navigation mark identification algorithm. The control was exerted on two parameters, the longitudinal velocity of the car and the deviation angle. The error to be corrected was monitored on real test images, saved in a database. The inputs of the controller are position and orientation errors representing the current lateral error to be corrected and predictive lateral error correction, respectively. The controller output was used to sharpen the outputs in order to reduce the computational cost of the algorithm. With this setup, the vehicle's reaction was quick as it approached the target line and longer as the vehicle moved further away from it to keep a proportionate level of precision and smoothness. Its performance was tested on a simulation of the multi-body model of the vehicle, on some trajectories (straight, circular, sinusoidal). In all scenarios, the controller was able to steer their vehicle with low lateral deviation and a natural feeling of steering. The addition of white noise allowed the controller to navigate successfully without apparent disturbance. The next step will be real experiments, and a vision system implemented in an economic platform for the detection algorithm. The findings show that this fuzzy system can be implemented as real time in some simple and cheap equipment. This could make it a realistic option for self-driving vehicles that can do different agricultural jobs.*

Keywords - *Fuzzy Control, Autonomous Vehicle, Tracking Control, Computer Vision, Precision Agriculture.*

1. Introduction

1.1. Precision Agriculture and Recent Developments

In order to achieve more optimal and efficient management of those elements, the so-called precision agriculture methods have been developed, which involve monitoring, analysing, and managing tools as well as technologies [1-4], providing better possibilities to farmers for using resources and increasing crop yield. It combines a number of tools like instead stakeholders in precision agriculture, such as Sensors and GPS devices or satellite Imageries, Drones, and Data Algorithms, providing informed decision-making based on the particular situation of each field as described above. The aim is to achieve the maximum production, with an eye on sustainability: the idea is to minimize both environmental impact and costs. In very simple terms, it is looking to use inputs more efficiently and to be much more responsive to the actual needs of farm crops. Precision Agriculture. It is an emerging higher form of farming. While the concept of precision agriculture sounds very promising, it still suffers from many challenges that prevent its adoption in most places. The most pronounced barrier is the fact that equipment and technology have high upfront costs. Furthermore, in many rural areas, the boarding strength of the internet or communication signal is weak, and operators are generally required to have certain training to operate on the systems or intelligently analyze the collected data [5-7]. Another barrier is the incompatibility between machines and sensors, as each device generally operates with its own format or communication protocol. These difficulties need to be overcome so that precision agriculture can reach its potential benefits, not only in academic research. Currently, many farms are using Global Navigation Satellite Systems

(GNSS) to map their fields and, at the same time, use it for guiding the tractor or autonomous robot on a centimeter level of precision. These systems have the advantage that they can achieve near centimeter-level accuracy when using Real-Time Kinematic (RTK) correction. But in an actual scenario, GNSS is not always ideal. Performance is based on special equipment and a strong signal that often degrades or becomes unreliable, in particular in hills or bad weather conditions [8-9].

Satellites and Unmanned Aerial Vehicles (UAVs) or Drones are now widely used for monitoring the crop's condition. Multispectral or even hypersectral images are acquired by these systems in order to assess the health of plants, monitor early onset of stress, and estimate yields. Satellites, which are cheaper and provide broader coverage, do not take images very often and can be impeded by cloud cover. Drones do offer much greater detail and can be deployed whenever it suits, although there is a catch. They require trained operators, their flight restrictions can be prohibitive, and they must be maintained regularly, which can make them pricier to operate.

The sensors (such as IoT sensors) that are installed in the fields, like soil moisture, temperature, nutrient level, and other indices related to cropping pattern, can be used for obtaining real-time data [10-14]. This could enable farmers to monitor their fields at all times and respond as soon as anything changes. One advantage of such technology is to avail fine control of regions in a field. But the rub is that these sensors must be calibrated, maintained consistently, and work on a dependable internet connection-still a rarity in many rural areas.

Another option is to use Variable-Rate Technology (VRT) that can deliver fertilizers, seeds, or pesticides only on the field where they are needed and reduce waste and environmental troubles [15-17]. However, reduced equipment cost and efficient farm scheduling are hindered by the cost of the infrastructure required and high-definition maps for the accurate definition of application zones. Next generation sensing and computing paradigms, such as Machine Learning (in particular deep learning) or big data for predicting plant behavior, Holonic approaches, Heterarchical, multicriteria control through combination with other types of digital twins to detect if anything goes wrong, to act, detecting any issue and act.

But though these methods are powerful, they rely on big and reliable databases and supercomputers that can do a lot of number crunching rapidly-things not every producer has. Autonomous ground-based navigation is one of the major breakthroughs toward full autonomous farming in recent years. It allows tractors, harvesters, and small agricultural robots to drive, navigate, and operate with limited human involvement [18-21]. These systems integrate prevalent technologies such as high-precision GNSS, RGB or multispectral cameras, LiDAR scanners, radar sensors, and advanced control and path-planning algorithms to work together. However, the practical on-farm deployment of these systems is a challenge. That is to say, the external environment varies greatly, and then the reliability of the system is hard to measure; Compatibility with high cost among all parts has also been a challenge for most farms based on present factories [24].

1.2. Multibody Modeling

Multibody system modeling. Multibody dynamics is a computational method to predict the motion of mechanical systems, where their interconnected parts are assembled at joints and subjected to external forces. Simply put, it describes the system as a set of interconnected rigid or occasionally flexible bodies. This approach allows analysing movements in detail - both translated and rotated ones - considering real working and environmental conditions [23]. In the domain of precision agriculture, ground navigation has been applied to autonomous vehicles [4], and interestingly, similar to our research, multibody modelling is known to have its importance from different aspects.

It provides the ability to simulate machine behaviour on any ground type (rocky or soft) while optionally being able to analyse suspension system movement, wheel traction/slide on soil, and load transfer in operation as well. The abstract model presented is highly recommended to validate new control law -example: Fuzzy Logic Control – guidance principle..- GNSS-based, apart from cost-effective and time-consuming field tests. Furthermore, the vehicle performance with varying soil type, crop row configuration, and operation speed can be investigated to optimize its stability while increasing path-following accuracy and reducing energy consumption towards a more responsive, even sustainable agriculture [24-26].

Integrating fuzzy control into unmanned ground navigation in the context of precision agriculture is an effective way for handling nonconstraints, uncertainties, and the diversity of field environments present under real environmental conditions [27-30].

“When you put it together with multibody modeling-this tells you how the vehicle’s mechanics and its interactions with soil work in detail-then the system not only simulates, but also predicts, and iteratively fine tunes, how it behaves across all manner of terrains and operatings,” This mix allows the vehicle to follow its path more accurately and safely-although with less effort, thanks in part to better anticipation for suspension movement, wheel slip or an uneven load on a trailer. It can be said that fuzzy control combined with multibody modeling provides an operational connection between the high-level control will and the physical behavior of an example farm machine when taking action during field operation.

1.3. Agricultural EV Multibody Model

In the present work, a multibody model of the modified EV concept developed to operate in farm conditions was introduced. The first step was to develop detailed elements consisting of the EV's structure and mechanics in Solid Works. Subsequently, the mentioned model was exported into MATLAB during the application of the Simscape-SimMechanics and analyzed under working conditions. Numerous scenarios were assumed to evaluate its performance and stability, as well as driveability.

The simulation route was based on the literature data, but was not developed accordingly. It was utilized in the current research to verify the suitability of autonomous guidance. As a result, the trajectory was not analyzed as rigorously as real-time values because previous studies validated the description's accuracy.

The combined methods allowed the analysis of the EV response to uneven terrain and provided general assumptions concerning autonomous precision farming.

1.4. Contributions and Novelty

The contributions of this paper include three features that set it apart from existing works on fuzzy control for AVs.

The controller uses singleton output responses, which are slightly "offset," providing a nonlinear characteristic: Fast recovery when the error signal is small, but adopts an increasingly smoother response as the error grows. This function of a steering system holds it on course while providing steadiness.

Second, the control was decomposed into two main parts: steering and speed control. This presented structure gives the possibility to the vehicle to maintain its balance even without using highly complex methods related to unstable conditions or sudden environmental changes.

Finally, the results showed that the controller is able to run in real time on minimal-cost embedded hardware. This also proves that sophisticated fuzzy control strategies are not necessarily limited to pricey systems and can work in small agricultural machines with low-performance processors.

2. Materials and Methods

2.1. Vision System and State Estimation

The vision system is built with a front-facing RGB camera rigidly positioned at the middle of the car's front chassis. It is 1.20 m above the ground and is angled down by around 25° - providing a clear, stable view of the crop rows ahead. The images are 2592 × 1728 pixels, with a rate of about 5 per second, which is more than adequate for slow agricultural motion, i.e., around the typical walking speed of ~3 km/h (or presumably lawnmowing).

(a)

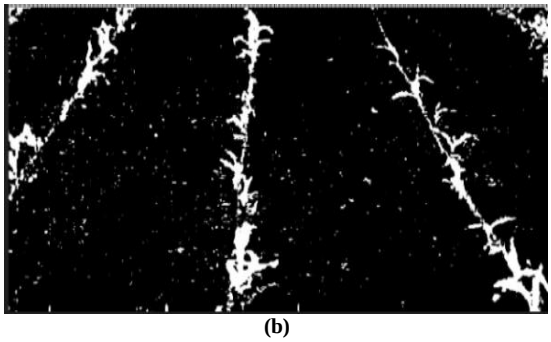

(b)

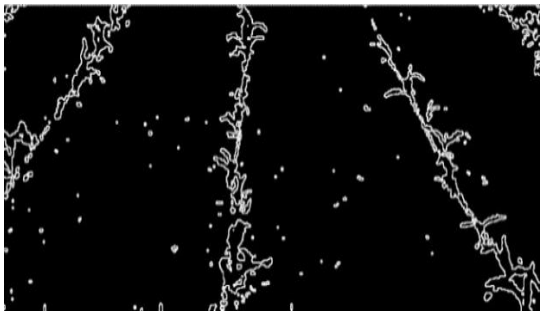

(c)

Fig. 1 Stages of preprocessing vision system: (a) Original RGB image of crop row, (b) Binary mask after green-channel enhanced and adaptive threshold is applied, and (c) Contours on the binary mask for the separation of vegetation lines.

2.1.1. Image Processing

The image processing pipeline- real-time run was implemented in C++ with the OpenCV library. That unfolds by way of a few main steps, executed one after the other:

- Perspective reduction: if the upper part of the image (+) contains perspective distortion, we crop it to leave only what is relevant for navigation.
- Spectral/space boost and grayscale conversion: converts the image to grayscale by enhancing the green channel, which is supposed to enhance vegetation and distinguish it from soil or background.
- Adaptive thresholding: an adaptive binarization is carried out in order to deal with varying light conditions, such as overcast or shadows between the plants.
- Morphological filtering: Opening and closing filters are used to remove small noise chunks, resulting in a clean binary mask that comprises only the mango area.

In Figure 1, the original image captured by the onboard camera is shown, followed by the cropped and thresholded version, and finally the processed image after edge detection.

2.1.2. Crop Raw Detection

The navigation line detection is the process of finding where the lane, which is indicated near the end of vision based on perception, should be used by the vehicle for automatic steering control. The system first performs pre-processing of the image, followed by segmentation, and detects vegetation contours that match crop rows, and provides a single navigation line, which is the desired route for the robot to travel.

The process includes the following steps:

- Contouring: In the second stage, the system detects green shapes, which are plants, based on these contours, and they are taken from a reprocessed binary image. A simple new row following method is applied to the indents, and it even works under changing light conditions or ground texture.
- ·Row center calculation: For each row of the image, it tests along which positions are the left and right limits of the crop area position (sweeping), and takes the middle point. You can already get a sense of where the navigation path should be by averaging all of those midpoints together.
- Smoothing and filtering: The unwrapped point can also jump a little due to noise, missing plants, or non-flat rows. We apply an average move in order to get a smoother-looking path, for it looks more like reality.
- Navigation line generation: in the end, a straight line is fitted over the filtered points set (first-order polynomial). The end-product is a seamless, blurred navigation line that remains distinct in the presence of gaps or leaf occlusion.

Here, the system combined all found crop rows into a single master navigation line, minimizing chatter to deliver good and robust guidance even on real-world, imperfect fields belonging to a customer; in other words, because the rows are not uniformly spaced or some of your plants failed out.

(a)

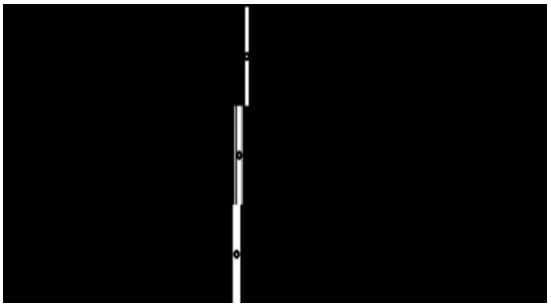

(b)

(c)

Fig. 2 Process of crop row detection: (a) Binary image where the central vegetation line is detected, (b) Blocks at which the crops are grown and centroids on these blocks, and (c) Original image with navigation line resulting from computation.

2.1.3. State Estimation: Lateral Position and Orientation

The two most important values we obtain from the navigation line are the lateral deviation (d) and orientation error (ϕ). To obtain d, the analysis focuses on the bottom of the image to measure the deviation of the detected line from the center. The center of the image is at the center of the vehicle and considered a point of origin. The pixels are converted into a distance in cm, applying a calibration factor. In that setup, resolution with 2592×1728 pixels extends over approximately 1.6 meters at the floor. The receding point was thus deduced from this correlation. To account for the small angle between the camera bank and scanner bed, we averaged these here-scaled values to approximately 0.08 cm/pixel. This calibration gives a useful value of about 85% of the data.

Sign convention:

- $d > 0 \rightarrow$ vehicle is to the left of the navigation line
- $d < 0 \rightarrow$ vehicle is to the right of the navigation line

Orientation error (ϕ) – Defined as the angle between the navigation line and the image vertical. Given the line's top and bottom points, ϕ is calculated from the slope via basic trigonometry.

Sign convention:

- $\phi > 0 \rightarrow$ line tilts to the right
- $\phi < 0 \rightarrow$ line tilts to the left

2.1.4. Robustness and Temporal Continuity

Temporal fallback. If the system can not find at least two centroids, it uses the navigation line of the previous frame so that the image does not jump all over, and does not make you do silly steering moves.

Calibrated scale. The scale is 0.08 cm/pixel, already taking into account a minor correction for the camera. This multiplier can be further changed after calibration adjustment with a grid on the field itself.

ROI adaptation. Cropping at the top of the image (on the third out) is saving a lot of "noise" and having a better signal that does not change according to the hour of the day.

2.2. Multibody Dynamic Modeling

The vehicle was modelled as a multibody system seeking to capture the interrelations between the chassis, wheel assemblies, steering linkages, and optional suspension features so that a level of complexity for control-in-the-loop simulations could be reached. The CAD model was modelled in SolidWorks and organized as subassemblies: chassis, front and rear wheels assembly, steering mechanism, and mounting systems. All the solid parts were exported from CAD with masses and inertias intact, and mechanical connections were turned into revolute joints (wheel rotation), universal joints (front wheel steer+spin), and rigid where it was appropriate. The model also maintained the geometric features of the system, so that by exclusion, simulation results would reproduce a statistical pattern of load transfer (Kinematic Fidelity) while feedforward was applied. Two frames are used: a world frame (X_w, Y_w) to report global pose and a body-fixed frame (X_b, Y_b) attached to the vehicle's center of gravity (CG) to express forces and velocities. This framing aligns with standard low-speed ground-vehicle practice and supports direct comparison against navigation states (X, Y, φ).

2.2.1 Longitudinal channel (Force Balance)

For straight-line and mild-curvature operation, the net force along the body x-axis is:

$$F_T = ma = F_{traction} - (F_{drag} + F_{rolling} + F_g) \quad (1)$$

with aerodynamic drag $F_{drag} = \frac{1}{2}\rho C_d A_f v^2$, soil rolling resistance modeled by a constant coefficient, and a gravity component acting on slopes. Example parameterization consistent with your prior setup is $\rho = 1.225 \frac{Kg}{m^3}$, $C_d = 0.64$, $A_f = 1.39\ m^2$, and $C_{rr} = 0.4$ for soil.

2.2.2. Lateral channel-kinematic bicycle (low-speed guidance)

Given the target operating speed (≈ 5 km/h), it is reasonable to neglect slip angles for guidance design and adopt the kinematic bicycle abstraction. Let $L = L_f + L_r$ be the wheelbase, δ_F The front steering angle, and V the forward speed. The kinematics are:

$$\dot{X} = V\cos(\varphi + \beta)$$

$$\dot{Y} = V\sin(\varphi + \beta) \quad (2)$$

$$\dot{\varphi} = \frac{V}{L}\tan(\delta_F)$$

With β, the vehicle slip angle (≈ 0 under the low-speed assumption). This model provides computational efficiency with sufficient accuracy for row-following control and for coupling with the perception module. The geometric relationship of slip angles and steering angles in the bicycle model is illustrated in Figure 3.

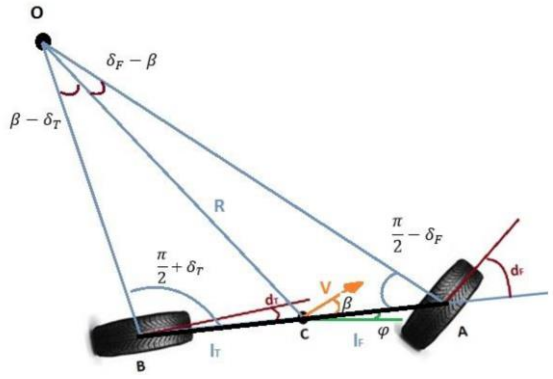

Fig. 3 Geometric representation of the dynamic bicycle model showing vehicle velocity V, yaw angle φ, slip angle β, front and rear slip angles δ_F, δ_T, wheelbase distances I_F, I_T and turning radius R.

2.2.3. Higher-fidelity Lateral Dynamics-Slip angles and Cornering Stiffness

When higher lateral fidelity is required (e.g., for faster maneuvers, abrupt curvature, or sensitivity studies), augment the model with tire slip angles and cornering stiffness to compute lateral tire forces at the front/rear. Using the dynamic bicycle with two DOF (y, r) (lateral translation and yaw), the governing equations are classically:

$$m(\dot{v}_y + V_r) = F_{y,f} + F_{y,r}$$

$$I_z\dot{r} = l_f F_{y,f} - l_r F_{y,r} \quad (3)$$

with linear tire relations near small slip:

$$F_{y,f} = C_f\alpha_f$$

$$F_{y,r} = C_r\alpha_r \quad (4)$$

Slip angles follow from geometry/kinematics, for small angles:

$$\alpha_f \approx \beta + \frac{l_f r}{V} - \delta_F$$

$$\alpha_f \approx \beta - \frac{l_r r}{V} \quad (4)$$

where β is the vehicle sideslip angle at the center of mass and δ_f The steering input at the front wheels. This extended formulation recovers the explicit understeer/oversteer tendencies and the transient coupling between lateral velocity and yaw dynamics.

The definitions of slip angles (α_f, α_r), sideslip angle β, lateral forces $F_{y,f}, F_{y,r}$, and related kinematics are illustrated in Figure 4.

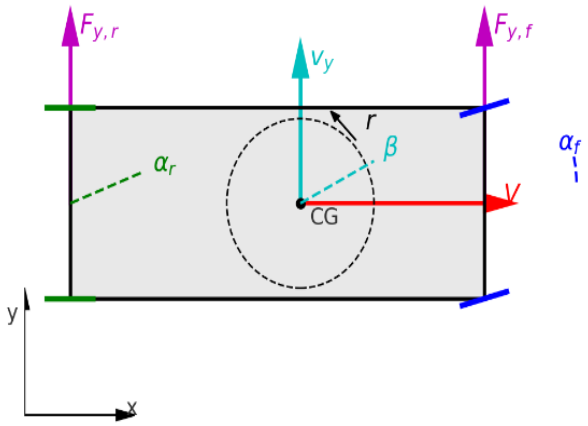

Fig. 4 Bicycle model scheme illustrating slip angles, sideslip, yaw rate, velocity components, and lateral forces

2.2.4. Compact Multibody Form (for completeness)

A compact descriptor that maps directly to your Simscape structure is:

$$M(q)\ddot{q} + C(q,\dot{q}) + G(q) = \tau \quad (5)$$

with q the generalized coordinates; M the mass matrix (from CAD inertias), C centrifugal/Coriolis and dissipative terms (incl. rolling), G gravity, and τ actuator/interaction forces.

2.2.5. Implementation in Simscape Multibody

The vehicle dynamic model has been generated using Simscape Multibody (a three-dimensional physical modeling tool that combines 3D mechanical multibody models with directly and fully coupled multidomain physical phenomena).

The vehicle CAD model was first brought to the environment Figure 5(a) as a geometrical and structural reference for the simulation. Based on this setup, the force transmission and motion parts were then established and linked together to simulate the dynamic response of the vehicle Figure 5(b).

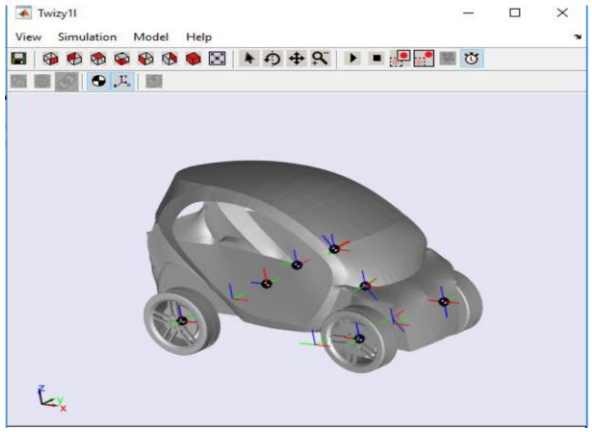

(a)

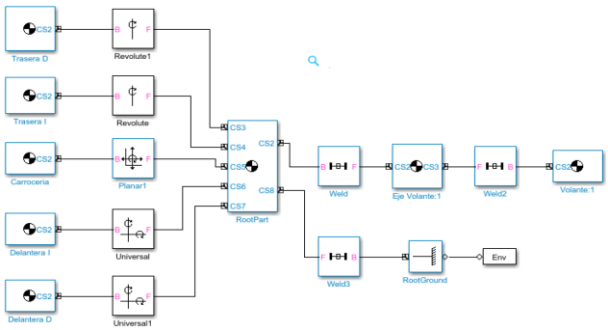

(b)

Fig. 5 (a)Imported CAD model of the vehicle, and (b)Assembly of joints.

The primary model was inserted in an environment set-up (Figure 6) which employed a Root Ground block and a basic planar joint. Once again, this setup means the vehicle is moving only on a horizontal plane, and thus the simulation is constrained to forward–backward and sideways movements. The initial position and speed were also added with a Joint Initial Condition block to ensure the system started in a stable and consistent way during the simulation.

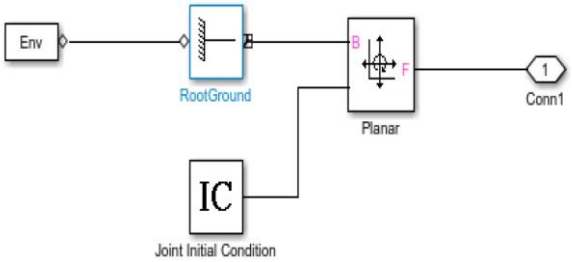

Fig. 6 Environment subsystem: constraint to the ground (Ground reference) and position, as well as velocity initialization

Sketch of the traction applied on rear wheels is presented in Figure 7. A velocity input is recorded, then integrated through motors acting on rotational joints. This allows the velocity input to be directly related to the rotation of the rear wheels and for output parameters such as wheel rotation and torque measurements.

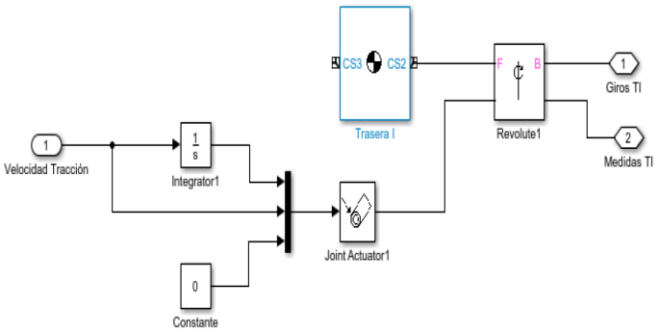

Fig. 7 Rear wheel subsystem: application of traction velocity through a joint actuator and measurement of angular variables

The two front wheels provide driving force and steering (Figure 8).

They are given the same forwarding speed as for the rear wheels, but the steering angle is regulated using a joint actuator subjected to steering commands. Moreover, a little lateral dynamics block was implemented, which computes the side velocity and estimates slip angles between the wheels during cornering. The driving power and the steering are both performed by the front wheels (Figure 8). They undergo forward motion in the same manner as the rear wheels, but they are steered by a joint actuator with input received from the steering signal.

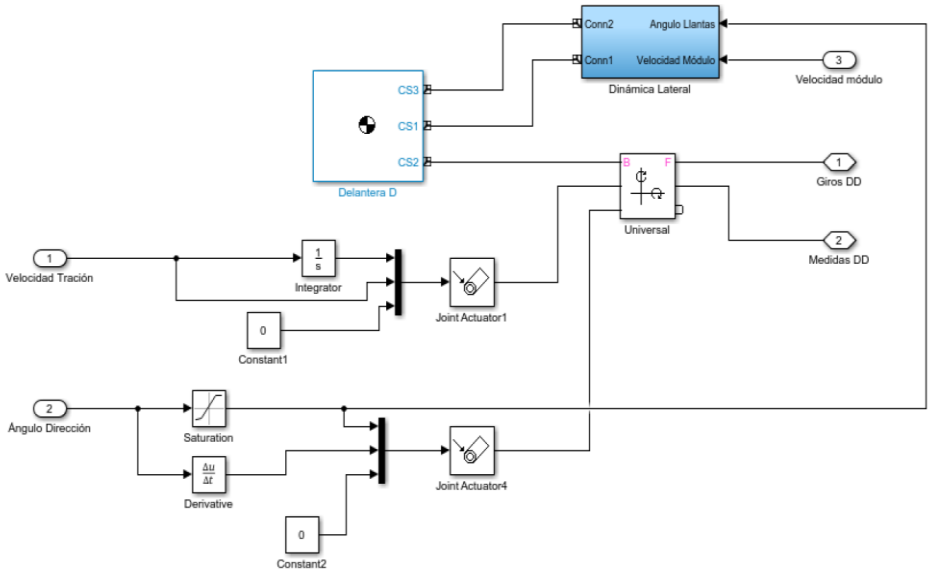

Fig. 8 Front wheel subsystem: integration of traction and steering inputs with lateral dynamics representation

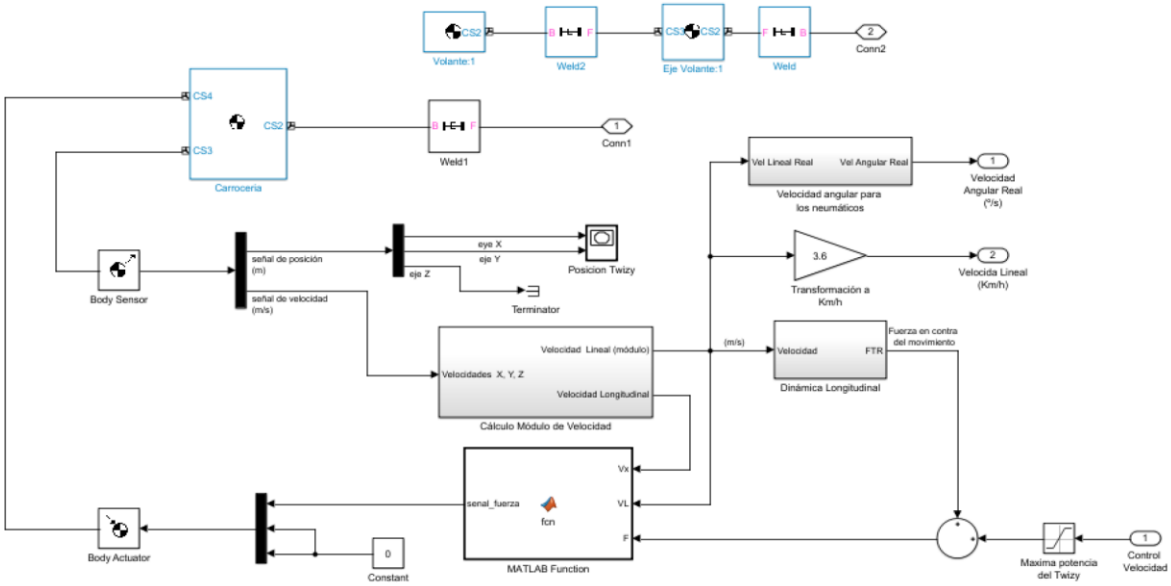

Fig. 9 Chassis subsystem: integration of vehicle kinematics, longitudinal dynamics, and energy limitation through power constraints

Furthermore, a lather dynamics block was added to calculate how the side velocity changes and to estimate the tire slip angles during corners. The backbone (ref. Figure 9) is the central structure to affix all subsystems. In the global referential, multiple rigid-body sensors are employed for measuring the vehicle's position and speed, whose readings will be used post-organization to estimate longitudinal velocity in km/h. These are then passed onto the longitudinal dynamics block, which takes into account all forces that partly or entirely slow down the vehicle, such as friction, rolling resistance, and aerodynamic drag. A MATLAB Function block was also included to connect the vehicle speed with thrust and maximum available power, such that the simulation reflects the energy constraints of a small electric car.

Finally, the loop of the entire dynamic model is closed with an actuator linked to the chassis, which applies external forces.

2.3. Fuzzy Controller Design and Implementation

The controller was developed based on a Mamdani-type fuzzy inference. The prime objective of this module is to force the unmanned agricultural vehicle that follows along the navigation line to stick back into its track whenever it comes off. The controller receives two inputs:

- The lateral error, $e(k)$, is simply the distance to the side of the vehicle (lateral position) from the center of the road.
- The error derivative, $\Delta e(k)$, which shows how fast that distance is changing over time-basically, whether the vehicle is starting to move away or coming back toward the line.

Thus, the set of inputs can be expressed as:

$$x(k) = \{e(k), \Delta e(k)\} \tag{6}$$

while the output of the system corresponds to the steering angle of the front wheels, denoted as:

$$u(k) = \delta_f(k) \tag{7}$$

where δ_f Regulates the magnitude of steering within the range $[-35°,\ 35°]$.

The input variables were represented using triangular membership functions, uniformly distributed around the origin to cover both small and large deviations. Figure 10 shows the membership functions for $e(k)$ and $\Delta e(k)$.

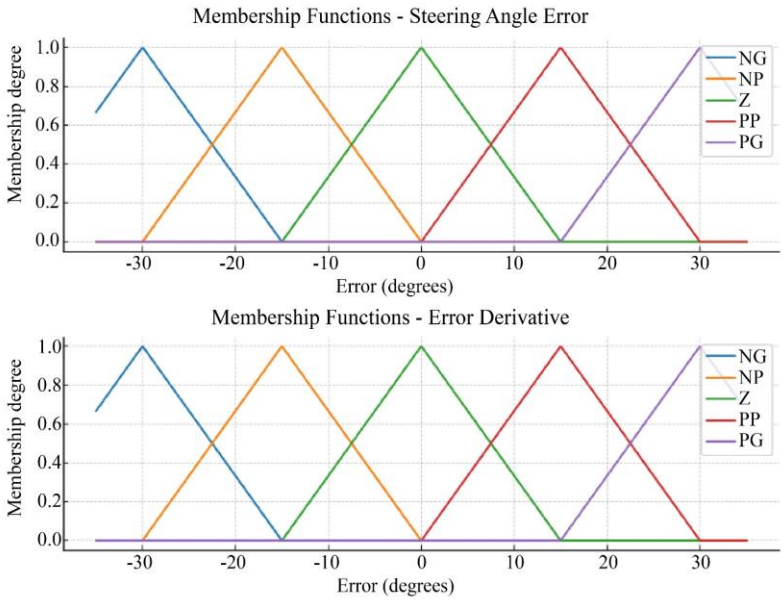

Fig. 10 Triangular membership functions for the fuzzy inputs: (a) lateral error (−35° to 35°), and (b) error derivative (−70°/s to 70°/s), with symmetric pairwise intersections at 0.5.

The rule base was formulated according to a heuristic scheme inspired by human operator experience:

$$R_i: IF\ e(k)\ is\ A_i\ AND\ \Delta e(k)\ is\ B_i\ THEN\ \delta_f\ is\ C_i$$

where A_i y B_i Are fuzzy sets of the inputs and C_i Are singleton-type output values.

In contrast to the continuous output function-based methods, this work used a discrete singleton. q_i, due to μ_i It directly corresponds to steering angles. The weighted average method was used to calculate global output:

$$\delta_f(k) = \frac{\sum_{j=1}^{N} u_j(x(k)) \cdot q_i}{\sum_{j=1}^{N} u_j(x(k)) \cdot q_i} \tag{8}$$

where:

- $u_j(x(k))$ is the activation degree of rule j.
- q_i Is the singleton output value associated with the rule.
- N is the total number of rules.

Figure 11 presents the singletons corresponding to different levels of angular correction.

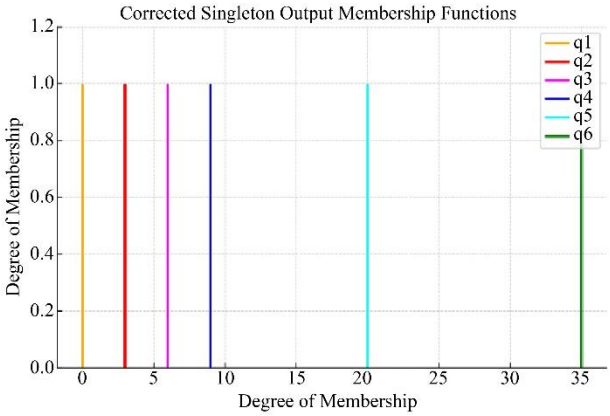

Fig. 11 Singleton output membership functions used in the fuzzy steering controller

For inducing more adaptive responses of the system, the singletons were non-symmetrically detuned with respect to their central positions. This introduces nonlinearity into the linear defuzzifier of the controller, and yields a nonproportional gain-controller.

That is, this special behavior comes in handy in reality.

- At zero error, the controller becomes very responsive – allowing for fast and accurate correction.
- However, that softening response prevents the reaction from overreacting, allowing the system as a whole to remain more stable.

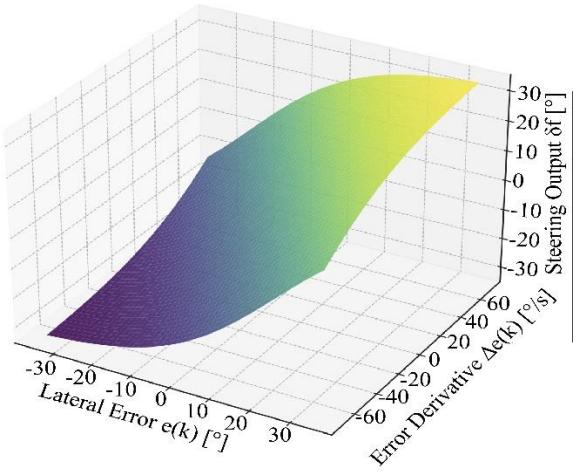

Fig. 12 Control surface of the fuzzy controller with inputs Error and Error Derivative and output Steering Output

This nonlinear effect is highlighted in Figure 12, in that the deformations of singletons sharply affect the behavior of the output surface. Another Mamdani-type fuzzy controller controlled the forward speed of the vehicle. Its concept is simple: slow the car down when there are large deviations and allow it to go faster when it is more or less steady and already well aligned with the trajectory. In addition to the lateral error $e(k)$ and $\Delta e(k)$, this controller also makes use of the orientation error $\theta_e(k)$ and its rate of change $\Delta\theta v$. That is, the control action does not just care how far away it is from the line, but also if it is pointed in a direction that moves us toward the right place. We can then represent the input vector as:

$$x(k) = \{e(k), \Delta e(k), \theta_e(k), \Delta\theta_e(k)\} \quad (9)$$

The output is the forward speed $v(k)$, represented by singleton values:

$$S = \{0, 0.5, 1, 1.5, 3, 6\}\ [Km/h] \quad (10)$$

Fuzzy rules regulating the speed of the vehicle were designed to adjust velocity based on how significant the combined errors are.

- When the lateral and orientation errors are both small, the system allows for faster vehicle movement, 3-6 km/h along the line while driving efficiently.
- In the case of minor deviations, the velocity decreases slightly so that it is between 1 and 1.5 km/h, letting you control your walking with little effort.
- In the case of more critical situations, where errors are huge, like big swerving or going off the right path due to a low CoG, even at low speeds (for instance, 0 - 0.5 km/h), the controller slows down the vehicle almost to a stop and keeps it stable without erratic responses, which compromise safety.

As with the steering controller, the singletons' outputs were shifted from the center. That slight variation has the defuzzification to behave non-linearly, smoothing the error values with respect to velocity. There are two important characteristics of the resulting control surface:

- The controller is effective, exhibiting very small errors around zero and making the car respond quickly and reasonably smoothly when arranged adequately.
- It softens when the deviations increase, so as to slow down in order not to make big corrections, but also stabilizes the motion.

4. Results and Discussion

4.1. Validation of Crop Row Detection

The task of serving the navigation data, which is required by the control part of the system, was managed by the

perception module. Two main signals were output in real-time: the lateral deviation between the vehicle and a navigation line (calculated from center to vehicle), and the angle between the heading of the vehicle and vertical reference Figure 2(c).

A number of trials were made on an actual drive, and the overall results are indicated in Table 1. As a final conclusion, the perception stage cleared the error out to acceptable levels for fuzzy control application 8% lateral distance and 6% angle overall). These values demonstrate that the perception navigation system changes smoothly without distraction from light or field conditions.

Table 1. Representative connection results of distance and angle in the perception stage

Sample	Distance (cm)	Angle (°)
1	-10.56	4.6903
2	-10.56	4.6903
3	-10.64	4.8522
4	-9.76	4.6903
5	-9.68	4.6903
6	-9.92	4.8522
7	-11.12	5.0141
8	-11.20	5.0141
9	-11.44	5.0141
10	-11.28	5.1760
11	-9.76	3.0141
12	-9.92	3.1760
13	-9.68	3.3380
14	-9.92	3.3380
15	-9.68	3.5000
16	-9.92	3.5000
17	-9.76	3.6619
18	-9.68	3.6619
19	-9.76	3.8238
20	-6.64	0.7742

The results indicate that the perception part of this system provides a stable and reliable foundation for subsequent fuzzy control.

3.2 Vehicle Multibody Simulation

Two open-loop steering maneuvers were used to study the kinematic and dynamic behaviour of the vehicle by employing the model presented in Simscape Multibody. As a result, the data demonstrates how the steering input determines vehicle movement in the XY plane.

Simulation Case 1: Initially, the car traveled in a straight line. Then, a turn was made by applying an input to steer, and after the turn was completed, the steering input returned to zero so that the car could traverse a straight path once again. The XY graph in Figure 13(a) looks like we would expect - a graceful sliding sideways and then the heading returning to its original state. Figure 13(b) shows the input plots for the steering. This simple experiment verifies that the model can make short steering changes and then subsequent stabilisation, which are functional capabilities in order to check control performance in robotic row-following navigation.

Simulation Case 2: In this test, a more complicated steering signal was employed to simulate the case that is required when the vehicle needs to avoid an object or change from one plant row to another. In Fig.14a, the vehicle took a left turn first, then drove straight for a short distance, and quite po lastly turned right to follow its original heading again. The steering plot in Figure 14(b) shows a similar behavior - one positive angle followed by a negative angle of about the same amount was evident.

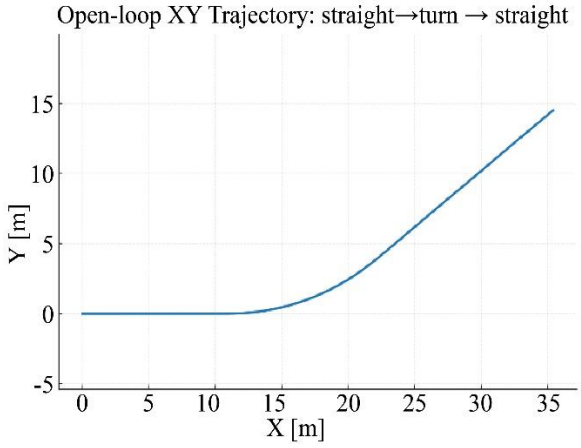

(a)

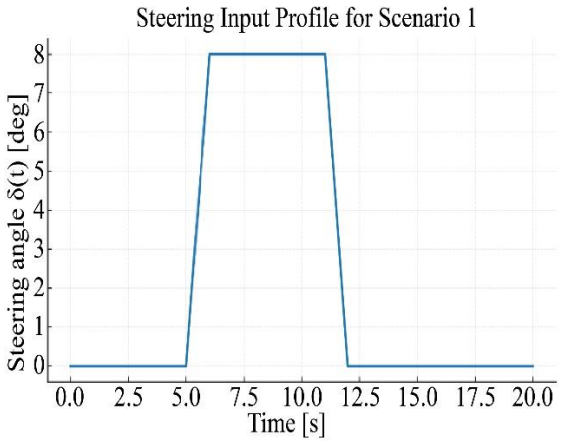

(b)

Fig. 13 Open-loop simulation of Scenario 1: (a) XY polar plot, and (b) steering input indicating one deflection-return-neutral movement.

There was also one other test drive, this time around the whole loop, to see how well the vehicle turns and what its minimum turning radius is. The model formed a smooth, continuous curve while the steering was constant, so that the circle must be stable and regular in XY view.

From these runs, two major findings can be concluded for the model. First, the smooth speed profile shows that this relationship between steering and forward motion is being accurately simulated -geometric consistency is granted through the simulation.

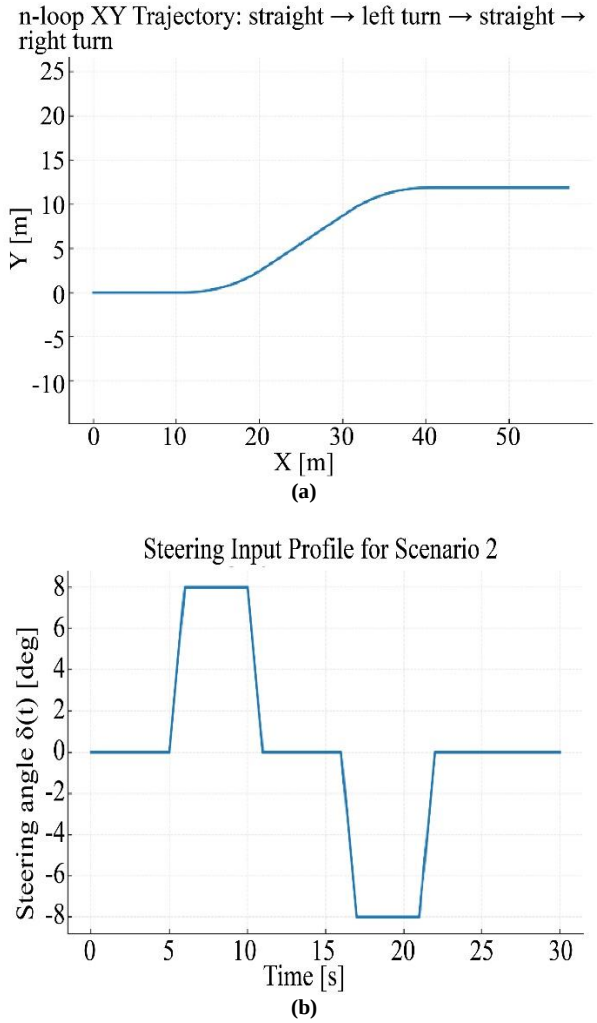

Fig. 14 Open-loop simulation of Scenario 2: (a) XY polar plot, and (b)steering input indicating one deflection–return-neutral movement

Second, this circular test helps figure out the real turning radius of the vehicle, which is an important value when designing path-planning and control methods for farm conditions.

3.3. Steering Control Performance

In order to validate the behaviour of the fuzzy steering controller, a straightforward experiment was conducted by the research team. The vehicle was pushed to follow a straight line, but it is tilted; some random white noise was added so that the situation appears a little more like in the real field (not perfect). Then the vehicle's black real trajectory, and red were points compared to the reference line Figure 16(a); and despite all that noise, the controller can hold the vehicle most of the time,/close to a reference, correcting slight drifts and avoiding those huge side errors which pop up sometimes. With respect to the perceived lateral error see Figure 16(b), it could be noted that the same were very contained during almost the entire experimental work. The root mean square error was only some 0.07 m, and the largest discrepancy did not exceed something like 0.18 m While these numbers are approximate, we see that the system stayed relatively stable.

In the end, tracking was easy and there were no weird oscillations, meaning that despite the obvious noise in measurements, the fuzzy controller actually maintained good precision! That sort of behavior is more or less what they had expected in a realistic field condition.

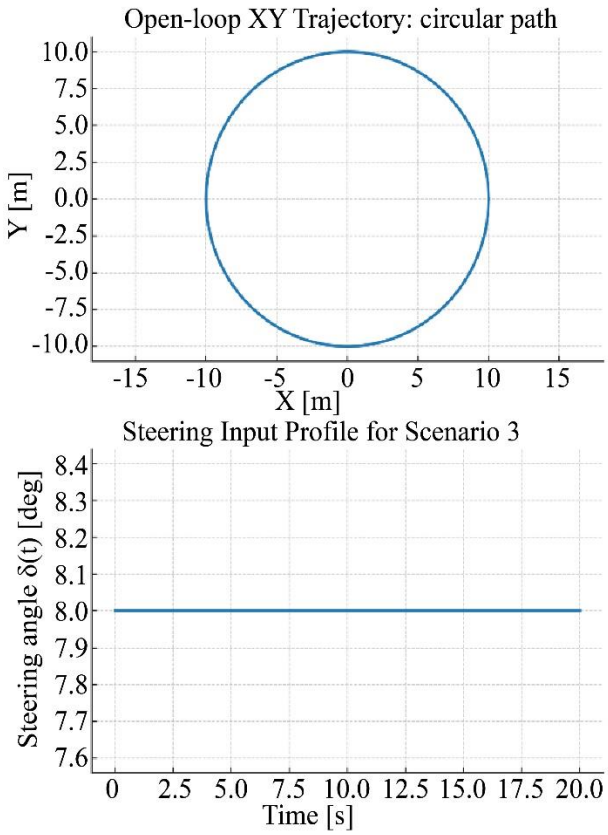

Fig. 15 Open-loop simulation of Scenario 3: (a) XY polar plot, and (b)steering input indicating one deflection–return-neutral movement.

The steering output of the controller (refer to Figure 16(c)) again proves the robustness of the system. The angle response is smooth - not weird oscillations here-so you can afford some outside perturbation or a minor bump without losing stability. The whole steering command throughout the test was about ±6.5°, which remained considerably below the limits of safe steerability of the vehicle. It is proven that the fuzzy controller maintains precision and at the same time is secured for the actuator. It followed a mixed path of straight, left turn, straight, and right turn in the second test. The reference and ground truth paths are depicted in Figure 17(a)),

the lateral error along the travelled route is shown in Figure 17(b), and the steering signal issued by its dedicated controller is presented in Figure 17(c).

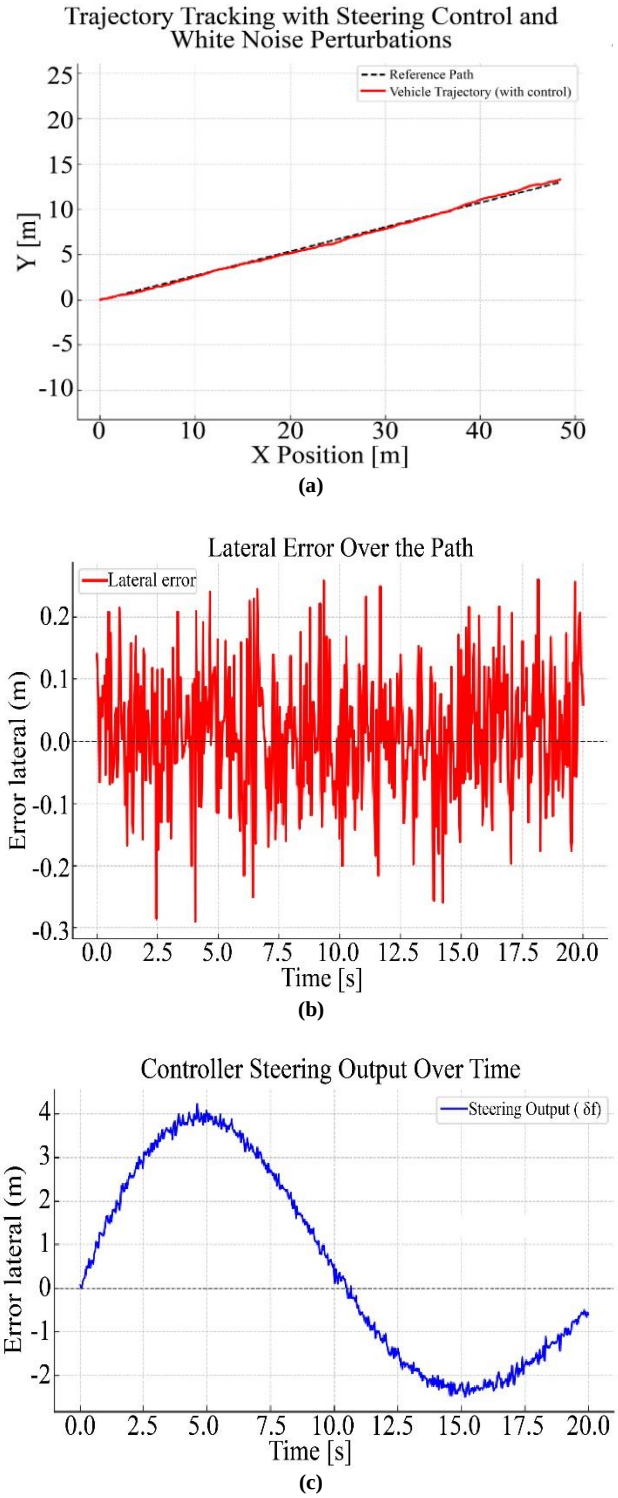

Fig. 16 Vehicle path tracking with white noise disturbances: (a) XY path versus the reference, (b) lateral error, and (c) steering control output.

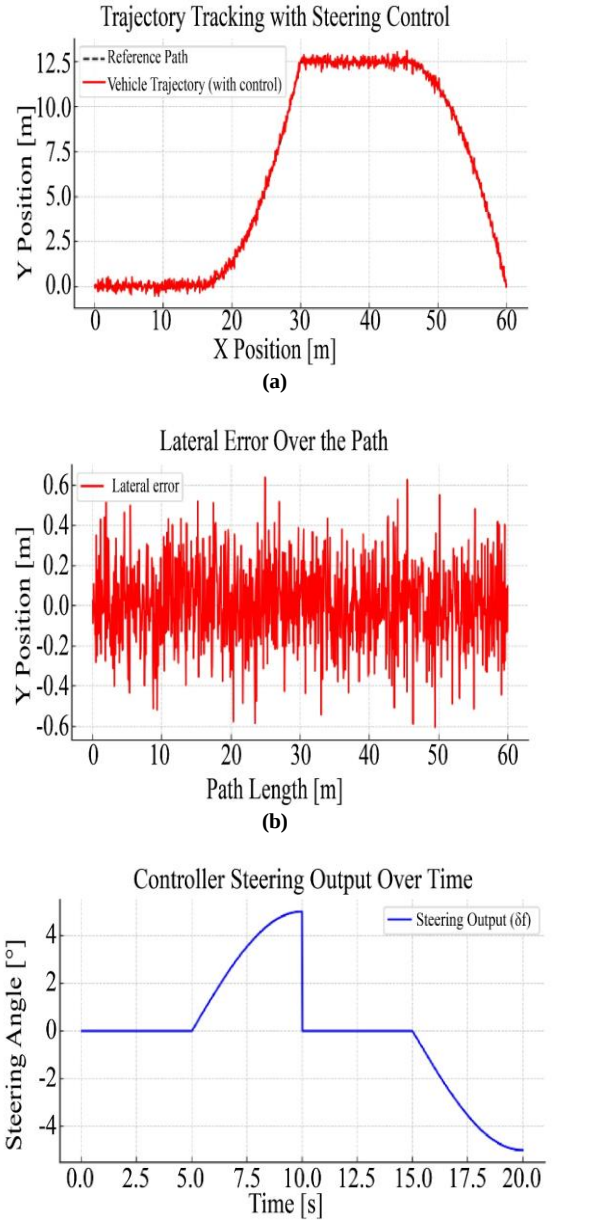

Fig. 17 Vehicle trajectory tracking, scenario 2, when subjected to white noise disturbances: (a)XY path vs. reference, (b)lateral error, and (c)steering control input.

The tests demonstrated that the controller was doing a good job of adhering the vehicle to near the line it was commanded to follow. If you do this, when the first curve comes, it will cause the steering to shift positively so that the car will turn to the left again, and then it returns to zero after becoming straight. Then the controller steered the other way, slightly in the negative direction, so the vehicle could negotiate a right turn to return to its normal pointing. Throughout the run, the side error remained relatively modest. The largest deviation from the reference line was smaller than 0.25 m, which is a good estimate. The errors were balanced-looking, too-the vehicle was not favoring one side over the

other, which meant that your control input was proportional in one direction and in the opposite direction. In other words, the system could take a path that makes left and right turns in random order, but not lose precision. Even when the path veered suddenly in one direction or the other, steering was smooth and stable enough to show that this controller should be up to at least real field conditions.

3.4. Discussion

Occasionally, you might get away with it, but forget about PID for the rest ofÂ your life while your system is nonlinear; otherwise, it is very inconvenient to tune them up. An example of that is your way steering systems, where your tire is to the ground, the terrain you are in, and the turning radius, which all change at all times. Type: Slow to clear (or even Intermittent PID) controller. Sometimes a PID gets too slow, and being itself based on a control loop that is rather old, it would still contain enough power to get unstable. But in this model, it is constructed not only by a fuzzy controller. It also follows rules to make various movements feel like how a human driver might respond, so that it takes smoother turns and makes speedier recovery, among other benefits. Another strong point is robustness.

There are no ideal straight rows in the field, and the light is not stable. They are the circumstances that confound autocratic bosses. The need for fuzzy logic to deal with uncertainty is based on gradual or 'soft' blending of decisions (versus abrupt transition). This means it can be very robustly applied to a car with some noise or information in its camera view. There are still some unresolved questions, however. Vision processing involves processing a lot of pictures per second, and this will be very stressful for small, albeit not really powerful, processors. The experiments are conducted on simulation only; however, the complete system needs to be validated in outdoor conditions where part of the camera view may be occluded with dust, vibration, or even with culture, which could have an impact on both perception and actuation. Even so, all in all, there is much to be hopeful about. And because it is being powered by cheap electronics, the machine could sit atop small and affordable farm vehicles. And that is important for small farmers, who are typically unable to invest in high-end automation systems. Refined and further experiments, this could perhaps bring delicate control to the dull machines of daily life in a realistic way.

4. Conclusion

This paper shows the interaction between a computer vision algorithm for crop row detection and its use as an autonomous navigation marker, and a non-analytical dynamic model of an autonomous vehicle for precision agriculture. Multibody modeling proves to be a practical and efficient tool in situations where obtaining analytical models is particularly complex, whether due to the number of components, the number of assumptions, or the mathematical cost. The multibody model is based on the intrinsic properties of each element, so by understanding its specificities, such as mass, dimensions, construction material, etc., an efficient and realistic model can be built.

As a technique that does not rely on an analytical model of a system, fuzzy control is an ideal strategy for this type of work, where the goal is to avoid obtaining an analytical model. This paper demonstrates that the control model using clear outputs offers important benefits, such as the nonlinearity of the control action. Finally, the work demonstrates that the integration of the three elements works correctly, allowing for the simulation of different operating scenarios for the agricultural vehicle. This allows us to propose future lines of work, such as physical implementation.

References

[1] George Mgendi, “Unlocking the Potential of Precision Agriculture: Benefits, Challenges, and Future Directions,” *Discover Agriculture*, vol. 2, no. 1, pp. 1-24, 2024. [CrossRef] [Google Scholar] [Publisher Link]

[2] Sofia Bahmutsky et al., “A Review of Life Cycle Impacts and Costs of Precision Agriculture for Field Crops,” *Sustainable Production and Consumption*, 2024. [CrossRef] [Google Scholar] [Publisher Link]

[3] Jiahui Xu et al., “The Evolution of Precision Agriculture and Food Safety,” *Frontiers in Sustainable Food Systems*, vol. 8, pp. 1-26, 2024. [CrossRef] [Google Scholar] [Publisher Link]

[4] James Lowenberg-DeBoer, and Bruce Erickson, “Setting the Record Straight on Precision Agriculture Adoption,” *Agronomy Journal*, vol. 111, no. 4, pp. 1552-1569, 2019. [CrossRef] [Google Scholar] [Publisher Link]

[5] Sofia Bahmutsky et al., “A Review of Life Cycle Impacts and Costs of Precision Agriculture for Field Crops,” *Sustainable Production and Consumption*, vol. 52, pp. 347-362, 2024. [CrossRef] [Google Scholar] [Publisher Link]

[6] Mary Sanyaolu, and Arkadiusz Sadowski, “The Role of Precision Agriculture Technologies in Enhancing Sustainable Agriculture,” *Sustainability*, vol. 16, no. 15, pp. 1-16, 2024. [CrossRef] [Google Scholar] [Publisher Link]

[7] Johannes Munz, “What if Precision Agriculture is Not Profitable?: A Comprehensive Analysis of the Right Timing for Exiting, Taking into Account Different Entry Options,” *Precision Agriculture*, vol. 25, pp. 1284-1323, 2024. [CrossRef] [Google Scholar] [Publisher Link]

[8] Dorijan Radočaj, Ivan Plaščak, and Mladen Jurišić, “Global Navigation Satellite Systems as State-of-the-Art Solutions in Precision Agriculture: A Review of Studies Indexed in the Web of Science,” *Agriculture*, vol. 13, no. 7, pp. 1-17, 2023. [CrossRef] [Google Scholar] [Publisher Link]

[9] Jing Guo et al., "Multi-GNSS Precise Point Positioning for Precision Agriculture," *Precision Agriculture*, vol. 19, no. 5, pp. 895-911, 2018. [CrossRef] [Google Scholar] [Publisher Link]

[10] Vijendra Kumar, "A Comprehensive Review on Smart and Sustainable Agriculture using IoT Technologies," *Smart Agricultural Technology*, vol. 8, pp. 1-22, 2024. [CrossRef] [Google Scholar] [Publisher Link]

[11] Sheikh Mansoor et al., "Integration of Smart Sensors and IoT in Precision Agriculture: Trends, Challenges and Future Perspectives," *Frontiers in Plant Science*, vol. 16, pp. 1-21, 2025. [CrossRef] [Google Scholar] [Publisher Link]

[12] Tymoteusz Miller et al., "The IoT and AI in Agriculture: The Time Is Now-A Systematic Review," *Sensors*, vol. 25, no. 12, pp. 1-32, 2025. [CrossRef] [Google Scholar] [Publisher Link]

[13] N.S. Abu et al., "Internet of Things Applications in Precision Agriculture: A Review," *Journal of Robotics and Control*, vol. 3, no. 3, pp. 338-347, 2022. [CrossRef] [Google Scholar] [Publisher Link]

[14] Gourab Saha et al., "Smart IoT-Driven Precision Agriculture: Land Mapping, Crop Prediction, and Irrigation System," *Plos One*, vol. 20, no. 3, pp. 1-33, 2025. [CrossRef] [Google Scholar] [Publisher Link]

[15] Gopal Tiwari et al., "Terrain-Integrated Soil Mapping Units (SMUs) for Precision Nutrient Management: A Case Study from Semi-Arid Tropics of India," *NDT-Journal of Non-Destructive Testing*, vol. 3, no. 3, pp. 1-17, 2025. [CrossRef] [Google Scholar] [Publisher Link]

[16] Robina Kousar et al., "Farm-Scale Soil Spatial Variability at a Mountain Research Farm Provides Basis for Precision Agriculture," *Scientific Reports*, vol. 15, no. 1, pp. 1-22, 2025. [CrossRef] [Google Scholar] [Publisher Link]

[17] Megha Sharma, Shailendra Goel, and Ani A. Elias, "Predictive Modeling of Soil Profiles for Precision Agriculture," *Scientific Reports*, vol. 15, no. 1, pp. 1-17, 2025. [CrossRef] [Google Scholar] [Publisher Link]

[18] Hongxuan Wu et al., "Review on Key Technologies for Autonomous Navigation in Field Agricultural Machinery," *Agriculture*, vol. 15, no. 12, pp. 1-28, 2025. [CrossRef] [Google Scholar] [Publisher Link]

[19] Md. Sabbir Hossain et al., "Automatic Navigation and Self-Driving Technology in Agricultural Machinery: A State-of-the-Art Systematic Review," *IEEE Access*, vol. 13, pp. 94370-94401, 2025. [CrossRef] [Google Scholar] [Publisher Link]

[20] Canicius Mwitta, and Glen C. Rains, "The Integration of GPS and Visual Navigation for Autonomous Navigation of an Ackerman Steering Mobile Robot in Cotton Fields," *Frontiers in Robotics and AI*, vol. 11, pp. 1-19, 2024. [CrossRef] [Google Scholar] [Publisher Link]

[21] Shivam K. Panda, Yongkyu Lee, and M. Khalid Jawed, "Agronav: Autonomous Navigation Framework for Agricultural Robots and Vehicles using Semantic Segmentation and Semantic Line Detection," *Proceedings of the IEEE/CVF Conference on Computer Vision and Pattern Recognition (CVPR) Workshops*, pp. 6272-6281, 2023. [Google Scholar] [Publisher Link]

[22] Zhixin Yao, Chunjiang Zhao, and Taihong Zhang, "Agricultural Machinery Automatic Navigation Technology-A Comprehensive Review," *Applied Sciences*, vol. 12, no. 13, pp. 1-20, 2023. [CrossRef] [Google Scholar] [Publisher Link]

[23] Andrea Grazioso et al., "Multibody Modeling of a New Wheel/Track Reconfigurable Locomotion System for Farming Vehicles," *Machines*, vol. 10, no. 12, pp. 1-29, 2022. [CrossRef] [Google Scholar] [Publisher Link]

[24] Filippo Califano et al., "Multibody Model for the Design of a Rover for Agricultural Applications: A Preliminary Study," *Machines*, vol. 10, no. 4, pp. 1-15, 2022. [CrossRef] [Google Scholar] [Publisher Link]

[25] Alessandro Febbraro et al., "Object-Oriented Modelling of a Tracked Vehicle for Agricultural Applications," *Computers and Electronics in Agriculture*, vol. 230, pp. 1-17, 2025. [CrossRef] [Google Scholar] [Publisher Link]

[26] Quanyu Wang et al., "Modelling and Control Methods in Path Tracking Control for Autonomous Agricultural Vehicles: A Review of State of the Art and Challenges," *Applied Sciences*, vol. 13, no. 12, pp. 1-22, 2023. [CrossRef] [Google Scholar] [Publisher Link]

[27] Rajan Prasad, Adesh Kumar Srivastava, and Rajinder Tiwari, "Fuzzy Logic-Based Sprinkler Controller for a Precision Irrigation System: A Case Study of Semi-Arid Regions in India," *Engineering Proceedings*, vol. 82, no. 1, pp. 1-12, 2024. [CrossRef] [Google Scholar] [Publisher Link]

[28] Abdennabi Morchid et al., "Fuzzy Logic-Based IoT System for Optimizing Irrigation with Cloud Computing: Enhancing Water Sustainability in Smart Agriculture," *Smart Agricultural Technology*, vol. 11, 2025. [CrossRef] [Google Scholar] [Publisher Link]

[29] Hayat Ait dahmad et al., "IT-2 Fuzzy Control and Behavioral Approach Navigation System for Holonomic 4WD/4WS Agricultural Robot," *International Journal of Computers Communications & Control*, vol. 19, no. 3, pp. 1-18, 2024. [CrossRef] [Google Scholar] [Publisher Link]

[30] Aylin Erdoğdu et al., "Combining Fuzzy Logic and Genetic Algorithms to Optimize Cost, Time and Quality in Modern Agriculture," *Sustainability*, vol. 17, no. 7, pp. 1-44, 2025. [CrossRef] [Google Scholar] [Publisher Link]

[31] MathWorks, Import SolidWorks Assemblies into Simscape Multibody, 2023. [Online]. Available: https://www.mathworks.com/videos/import-solidworks-assemblies-into-simscape-multibody-1701670328083.html

[32] MathWorks Documentation, SolidWorks-MATLAB & Simulink, 2025. [Online]. Available: https://www.mathworks.com/help/smlink/solidworks.html

[33] Jean Marie Lauhic Ndong Mezui et al., "SolidWorks/Simscape Multibody Co-Simulation of the Dynamic Model of a Mobile Manipulator System," *International Journal of Research in Engineering, Science and Management*, vol. 6, no. 1, pp. 1-9, 2023. [Google Scholar] [Publisher Link]